Published in final edited form as:
Pacing Clin Electrophysiol. 2010 March ; 33(3): 274–285. doi:10.1111/j.1540-8159.2009.02642.x.

Dual Variation in SCN5A and CACNB2b Underlies the Development of Cardiac Conduction Disease without Brugada Syndrome

Dan Hu, MD, PhD[*,1], **Hector Barajas-Martinez, PhD**[*,1], **Vladislav V. Nesterenko, PhD**[1], **Ryan Pfeiffer, BS**[1], **Alejandra Guerchicoff, PhD**[1], **Jonathan M. Cordeiro, PhD**[1], **Anne B. Curtis, MD**[2], **Guido D. Pollevick, PhD**[1], **Yuesheng Wu, MD**[1], **Elena Burashnikov, BS**[1], and **Charles Antzelevitch, PhD**[1]

[1]Masonic Medical Research Laboratory, Utica, New York, USA

[2]University of South Florida, Tampa, Florida, USA

Abstract

Background—Inherited loss of function mutations in *SCN5A* have been linked to overlapping syndromes including cardiac conduction disease and Brugada syndrome (BrS). The mechanisms responsible for the development of one without the other are poorly understood.

Methods—Direct sequencing was performed in a family with cardiac conduction disease. Wild-type (WT) and mutant channels were expressed in TSA201 cells for electrophysiological study. Green fluorescent protein (GFP)-fused WT or mutant genes were used to assess channel trafficking.

Results—A novel *SCN5A* mutation, P1008S, was identified in all family members displaying 1st degree atrioventricular block, but not in unaffected family members nor in 430 reference alleles. Peak P1008S current was 11.77% of WT ($p<0.001$). Confocal microscopy showed that WT channels tagged with GFP were localized on the cell surface, whereas GFP-tagged P1008S channels remained trapped in intracellular organelles. Trafficking could be rescued by incubation at room temperature, but not by incubation with mexiletine (300μM) at 37°C. We also identified a novel polymorphism (D601E) in *CACNB2b* that slowed inactivation of L-type calcium current (I_{Ca}), significantly increased total charge. Using the Luo-Rudy action potential model, we show that the reduction in I_{Na} can cause loss of the right ventricular epicardial action potential (AP) dome in the absence but not in the presence of the slowed inactivation of I_{Ca}. Slowed conduction was present in both cases.

Conclusions—Our results suggest genetic variations leading to a loss-of-function in I_{Na} coupled with a gain of function in I_{Ca} may underlie the development of cardiac conduction disease without BrS.

Keywords

Conduction Disease; Sodium Channel; Calcium Channel; Protein Trafficking

Address for editorial correspondence and reprint requests: Charles Antzelevitch, PhD, FACC, FAHA, FHRS, Gordon K. Moe Scholar, Masonic Medical Research Laboratory, 2150 Bleecker Street, Utica, New York, U.S.A. 13501-1787, Phone: (315) 735-2217, FAX: (315) 735-5648, ca@mmrl.edu.
[*]Authors contributed equally to this manuscript.

INTRODUCTION

Mutations in *SCN5A*, encoding the α-subunit of the human cardiac sodium channel ($hNa_v1.5$), have been reported to cause overlapping syndromes including Brugada syndrome (BrS)1, LQT3 form of the long-QT syndrome2, cardiac conduction disease (CCD, also referred to as Lev-Lenègre disease)3, congenital sick sinus syndrome (SSS)4, and/or atrial fibrillation5, that can manifest individually or together.6¯9

Cardiac conduction disease is characterized by an age-related impairment of conduction of the cardiac impulse across the atrioventricular node (AVN) and/or His-Purkinje system, leading to complete atrioventricular (AV) block, but without BrS-like ST-segment elevation. 3 These patients may present with syncope or sudden death, necessitating implantation of a pacemaker or. Right or left bundle branch block (R/LBBB) and broadening of the PR interval, QRS-complex, and QT interval are commonly observed. *SCN5A* mutations have been linked to cardiac conduction disease, allowing for genotype-phenotype correlation, yet a clear mechanistic understanding and approach to therapy is lacking.

BrS has previously been associated with mutations in seven different genes including *SCN5A* ($Na_v1.5$, BrS1)1, *GPD1L* (BrS2)10, *CACNA1C* ($Ca_v1.2$, BrS3)11, *CACNB2b* ($Ca_v\beta2b$, BrS4)11, *SCN1B* ($Na_v\beta_1$, BrS5)12, *KCNE3* (MiRP2; BrS6)13 and *SCN3B* ($Na_v\beta3$, BrS7) 14 that when expressed lead to a loss of function of either sodium (I_{Na}) or L-type calcium (I_{Ca}) channel current or to a gain of function of transient outward current (I_{to}). Experimental studies have demonstrated that inhibition of either I_{Na} or I_{Ca} or a combination of the two inward currents can induce a BrS phenotype.15, 16

Whereas loss of function mutations in SCN5A often result in both BrS and some level of cardiac conduction disease, in some cases the latter is manifest without BrS.17¯19 The mechanisms underlying the manifestation of cardiac conduction disease without BrS in cases of SCN5A loss of function mutations have largely eluded investigators thus far.

Herfst and colleagues showed that a trafficking defect may underlie *SCN5A* mutation-related loss of function associated with conduction defects20, but unlike BrS and LQT3, no study to our knowledge has identified a means to rescue *SCN5A* mutation-induced trafficking defects responsible for conduction problems. The present study identifies a novel missense mutation in *SCN5A* in a family with 1st degree AV block and demonstrates that loss of function is secondary to a trafficking defect that is amenable to rescue by exposure to low temperatures. Moreover, we have identified a second variation involving *CACNB2b*, which encodes the β subunit of the L-type calcium channel. This polymorphism, D601E, is shown to slow inactivation of I_{Ca} leading to a gain of function. Our data suggest that the dual genetic variation in inward current genes, causing a loss of function in I_{Na} coupled with a gain of function in I_{Ca}, underlies the development of cardiac conduction disease without BrS.

METHODS

Clinical Subjects

The study was approved by the Regional Institutional Review Board. All members of the immediate family underwent clinical and genetic studies after obtaining informed consent. The proband underwent Holter monitoring as well as an exercise stress test. P-wave duration, PR-interval, QT-interval, rate-corrected QT-interval and QRS-duration were measured from 12-lead electrocardiograms (ECG)s.

Mutation Analysis

Genomic DNA was extracted from peripheral blood leukocytes using a commercial kit (Gentra System, Puregene, Valencia, CA, USA). All exons and intron borders of *SCN5A* ($Na_v1.5$), *KCNE1* (MinK), *KCNE2* (MiRP1), *KCNE3* (MiRP2), *KCNQ1* (KvLQT1), *KCNH2* (hERG), *KCNA4* ($K_v1.4$), *KCND3* ($K_v4.3$), *KCNIP2* (KChIP2), *CACNA1C* ($Ca_v1.2$), *CACNB2b* ($Ca_vβ2b$), and *CACNA2D1* ($Ca_vα2δ1$), *IRX5, DDP10* genes were amplified and directly sequenced from both directions with the use of an ABI PRISM 3100-Avant Automatic DNA sequencer (Applied Biosystems, Foster City, CA, USA). To determine the prevalence of the nucleotide variations in the same ethnic population, genomic DNA from 430 ethnically-matched healthy reference alleles was used as control. The following SCN5A and *CACNB2b* primers were used for screening of family members:

SCN5A	
Exon 17- Sense	5'-GTCAAGCGGACCACCTGG-3'
Exon 17- Antisense	5'-CACACACACGGGCTCTGG-3'
CACNB2b	
Exon 13b- Sense	5'-GACTCTGCCTACGTAGAGC-3'
Exon 13b- Antisense	5'-CACATATGATTGCAGTGTAGAC-3'

Site-Directed Mutagenesis, Transfection and Electrophysiology Study

The ion channel variants were cloned by site-directed mutagenesis, expressed in TSA201 cells and studied using whole cell patch clamp techniques as detailed in the online supplement.

Localization of Sodium Channel

We assessed channel trafficking using Na^+ channels tagged with GFP, as previously described.11 Confocal microscopy was used to localize the channels and identify trafficking defects. (See online supplement for details)

Mathematical Model

Propagated action potentials (APs) were simulated using the Luo-Rudy 2 model21, 22 to which an robust I_{to} was added.23 (See online supplement for details)

Statistical Analysis

Data are expressed as Mean ± SEM. Two-tailed Student's t-test or ANOVA coupled with Newman-Keuls test were used for statistical analysis, as appropriate (SigmaStat, Jandel Scientific Software, Richmond, CA, USA). Differences were considered statistically significant at a value of $P<0.05$.

RESULTS

Clinical Observations

Affected family members were identified on the basis of generalized conduction defects (Table 1). The pedigree is shown in Figure 1. In the fall of 2004, the proband (**II-1**), 47 years old very fit male, presented in the emergency room after passing out at work. His younger daughter (**III-2**) was symptomatic with a reported "racing heart" during or following vigorous exercise. The proband and his two daughters (13 and 15 years old) underwent Holter monitoring and a treadmill stress test. The proband showed a pronounced first-degree AV block and an incomplete right bundle branch block (IRBBB), which were more pronounced during and after the exercise stress test (**II-1** in Figure 2A–C). A bifid T

wave and slight QTc prolongation were also observed during the exercise stress test (Figure 2B). His PR-interval varied between 300 and 360 ms at rest. The presence of a generalized conduction defect was also reflected in the longer than normal P wave and QRS duration (Table 1). Procainamide challenge failed to induce a BrS-like ECG (data not shown). Moreover, raising the position of the right precordial leads 2 intercostal spaces failed to reveal a BrS-ECG phenotype also. An ICD was implanted in the proband because of the unexplained syncope and a family history of sudden cardiac death.

The proband's sister (**II-3**) was 26 years old when she died of sudden cardiac arrest (21 years ago). The proband's daughters, 15 and 13 years of age, displayed sinus arrhythmia, bradycardia and PR intervals of 178 and 224 ms, which are prolonged for their age24 (**III-1 and 2;** Figures 2D and 2E). One of the daughters had a mild form of epilepsy **(III-2)**. The proband's brother, mother and two nieces displayed a normal ECG.

Molecular Genetics

Polymerase chain reaction (PCR)-based sequencing analysis revealed a double peak in the sequence of exon 17 of *SCN5A* (C to T transition at nucleotide 3022), predicting substitution of proline by serine at codon 1008 (P1008S) in all family members displaying ECG conduction defects. The novel missense mutation is located in the intracellular linker between domains II and III of *SCN5A*. The nucleotide change was not observed in 430 reference alleles (215 healthy race-matched individuals). Because of the appearance of bifid T waves and slight QTc prolongation during the exercise stress test, the proband was also screened for variations in other genes mentioned above. A heterozygous T1803G transition in exon 13, that predicted a substitution of aspartate for glutamate at position 601 (D601E) of *CACNB2b*, was present in 23% of ethnically matched controls. This polymorphism is located downstream of the β-subunit interaction domain segment. The polymorphism was detected in the proband (**II-1**) and one of his daughters (**III-1**).

Electrophysiological Characteristics of the *SCN5A*-P1008S Mutation

SCN5A-P1008S mutant and wild type (WT) sodium channels were co-expressed with *SCN1B* in TSA201 cells to assess the effects of the mutation on sodium channel function. The I–V relationships shown in Figure 3C demonstrate a major loss of function with peak I_{Na} density of P1008S reduced to 11.77 % of WT. Steady-state inactivation was measured by varying the conditioning pulse between −140 mV and −60 mV to inactivate the channels followed by a test pulse to −20 mV (Figure 3A). Half-inactivation voltage ($V_{1/2}$) and the slope factor of P1008S were not significantly different (Figure 3D). Recovery from inactivation evaluated using a standard double paired-pulse protocol showed that P1008S channels recover more slowly at very brief interpulse intervals (<20 ms) (Figure 3B and 3E).

To evaluate whether the loss of function caused by the P1008S mutation was due in part to a trafficking defect, we studied WT and P1008S channels tagged with fusion green fluorescent protein (GFP). XYZ scans of WT channels on the confocal microscope revealed both a central and peripheral pattern of staining, suggesting localization of the channel in the cell membrane as well as intracellular organelles (Figure 4A). In contrast, P1008S channel fluorescence was limited to intracellular organelles (Figure 4B), suggesting that channels were trapped in the endoplasmic reticulum and/or Golgi complex.

Previous studies have reported that trafficking of defective channels can be rescued by a variety of methods including incubation at low temperature and addition of pharmacological agents to the culture media25. Recent reports showed the effect of mexiletine, a Class I antiarrhythmic agent, to rescue trafficking-defective channels26. We evaluated the effect of both room temperature (RT), 22°C and mexiletine 300 μM. Incubation of the P1008S

transfected cells with 300 μM mexiletine for 48 hours did not rescue the trafficking defective channels (Figure 4C). However, incubation of the P1008S mutant channels at RT for 48 hours re-established both central and peripheral staining, suggesting restoration of normal trafficking of the channels to the cell membrane (Figure 4D). The peripheral:total fluorescence ratio was similar for WT and P1008S incubated at RT (0.572±0.036 and 0.545±0.030, n=8 for each), but much smaller for P1008S and P1008S incubated with Mexiletine (0.247±0.037 and 0.341±0.058, $P<0.05$ compared with WT, n=8 for each).

In another series of experiments, we examined the effect of incubation at RT or with mexiletine on functional expression of I_{Na}. Figure 5 shows the effect of incubation of cells transfected with P1008S *SCN5A* at RT in 48 hrs or incubation with 300 μM mexiletine in 48 hrs. Incubation with 300 μM mexiletine at 37°C failed to rescue expression of P1008S mutant channels, whereas incubation at RT for 24–48 hrs restored robust inward currents, consistent with the confocal results demonstrating rescue of the trafficking deficient channels.

Electrophysiological Characteristics of the *CACNB2b*-D601E Polymorphism

To determine the contribution of calcium polymorphism to the clinical phenotype, we expressed the WT and mutated *CACNB2b* constructs in TSA201 cells with *CACNA1c* and *CACNA2D1* and performed patch-clamp experiments (Figure 6A). The current density-voltage (I–V) relationship between WT and D601E channels was compared. A set of depolarizing pulses applied in 10-mV increments from a holding potential of −90 mV elicited robust I_{Ca} currents (Figure 6B). At 0 mV, the D601E variation in *CACNB2b* caused a slowing of inactivation: the time constant of the slow component of decay of I_{Ca} (τ_s) increased from 134.5 ± 11.0 in WT (n=9) to 168.8 ± 13.6 ms in D601E channels (n=7; $P<0.01$). The time constant of the fast component was not significantly altered (τ_f = 24.8 ± 2.1 ms for WT, n=9; τ_f = 24.0 ± 1.5 ms for D601E, n=7; $P>0.05$). This was accompanied by an increase in I_{Ca} density, which was statistically significant 50 and 300 ms into the pulse. (Figure 6C). The total charge carried by I_{Ca}, estimated as the area under the current trace recorded at 0 mV, increased by 144.3% (from 21.0±5.4 nC to 51.3±1.0 nC; n=9 for WT; n=7 for D601E; $P<0.05$).

Simulation Results

To assess the influence of the P1008S mutation in *SCN5A* alone and in combination with the D601E polymorphism in *CACNB2b* on the shape of the cardiac AP we simulated propagated right ventricular APs in a 1 cm cable. Figure 7 shows simulated APs under steady-state conditions (9^{th} and 10^{th} cycles) at BCL of 1000 msec. Maximal conductance of I_{to} was set to 2.2 mS/pF to simulate a right ventricular epicardial AP with a prominent spike-and-dome morphology (Figure 7A). When maximal conductance of fast I_{Na} was reduced to 35% of WT model to simulate the *SCN5A* defect, phase 0 overshoot decreased from +11.4 mV to −8.7 mV, conduction velocity slowed from 61 to 40 cm/sec (66% of WT) and the dome of the right ventricular epicardial action potential was lost (Figure 7B), consistent with the cellular changes associated with the development of Brugada syndrome.18 A decrease of the rate of voltage-dependent inactivation of $I_{Ca,L}$ to 85% of WT, simulating the change produced by the D601E polymorphism in *CACNB2b* (Figure 7C), resulted in restoration of the dome of the simulated right ventricular epicardial AP, indicating that this gain of function of I_{Ca} can prevent loss of the AP dome and thus prevent the development of the substrate for Brugada syndrome.

DISCUSSION

Clinical Correlation

We report a novel heterozygous missense mutation in *SCN5A* (P1008S) associated with a mild conduction defect in a family with a history of sudden cardiac death. The mutation is shown to cause loss of proper transport and reduced functional expression of *SCN5A*, capable of being rescued by exposure to low temperatures. ECG manifestations of impaired conduction in affected patients included prolonged P wave, QRS duration and PR intervals as well as incomplete RBBB, sinus arrhythmias and bradycardia, all likely due to loss of sodium channel function.

Numerous studies have identified mutations in *SCN5A*.3 Impaired atrioventricular conduction is the most common conduction problem identified, usually as an autosomal dominant trait.

Electrophysiology

Most mutations associated with cardiac conduction disease are functional, exhibiting complex biophysical properties predicted to reduce channel availability, such as altered voltage-dependence of activation, more rapid fast inactivation or closed-state inactivation, or enhanced slow inactivation.27, 28 Tan and colleagues described an *SCN5A* mutation related to cardiac conduction disease, displaying changes in inactivation kinetics, although whole-cell Na^+ current density remained unchanged.27 A loss of function mutation due to impaired protein trafficking has previously been associated with cardiac conduction disease, although a means of rescue was not identified in that study.20

In our study, the most striking feature of the P1008S channel was the severe reduction in I_{Na} amplitude. This loss of function is due to impaired trafficking since confocal microscopy revealed that P1008S channels fail to reach the plasma membrane. Patients with this mutation would be expected to have significantly reduced channel expression and consequently a reduced I_{Na}, which would be expected to reduce depolarizing current and excitability and thus account for the observed phenotype.29

Another possible contributor to the manifestation of the phenotype is the development of structural changes, as suggested by a recent $SCN5A^{+/-}$ mouse model which recapitulates the cardiac conduction disease phenotype. $SCN5A^{+/-}$ mice displayed progressive impairment of atrial and ventricular conduction associated with myocardial rearrangements and fibrosis. These conduction and structural abnormalities become more accentuated with advancing age.3, 30 It is noteworthy that in our P1008S family, the degree of conduction impairment was much more pronounced in the older member of the family (father). Association between degenerative abnormalities of the specialized conduction system and *SCN5A* loss of function has been demonstrated by Bezzina and co-workers in a case of compound heterozygosity.31

Loss of function mutations are often associated with BrS, although a number of previous studies have reported alleles exhibiting loss-of-function that are associated with cardiac conduction disease, without any manifestation of BrS.20, 27 The factors that determine the predominance of one phenotype over another are currently not well understood. The well-known clinical factors that may affect phenotypic expression include sex, age, and body temperature.19;32, 33 Genetic modifiers involve compound mutations34, spliced variant of *SCN5A*35, and a combination of polymorphisms.36 The disease penetrance also relate to humoral regulation, participation of auxiliary subunits, chaperone proteins, anchoring proteins and transcriptional factors.37

It is well known that the BrS phenotype is 8 to 10 times more prevalent in males versus females38, but sex-related difference among cardiac conduction disease patients is unknown. In one reported family manifesting both BrS and cardiac conduction disease, the phenotype appeared to be divided along gender lines. Four of 4 patients with BrS were males, whereas 6 of 7 progressive cardiac conduction disease patients were female.39 The presence of a more prominent I_{to}-mediated notch in the epicardium of males is thought to predispose males to the development of the Brugada phenotype, whereas a smaller epicardial notch in females protects them from BrS, but relegates them to development of cardiac conduction disease under conditions in which inward currents are compromised.40 A less dramatic outward shift in the balance of current active during the early phase of the action potential is thought to underlie the milder BrS phenotype in females.

In the present study, both male and female patients displayed the cardiac conduction disease phenotype, but none displayed the BrS phenotype, even when the right precordial leads were raised two intercostal spaces.33 The presence of a gain of function variation in *CACNB2b* leading to an increase in I_{Ca} likely underlies this unique phenotype. An increase in I_{Ca} mediated by administration of β adrenergic agonists or type 3 phosphodiesterase inhibitors such as cilostazol have been shown to suppress the BrS phenotype in both clinical and experimental studies. Augmentation of I_{Ca} prevents loss of action potential dome or restores the dome, thus preventing the development of ST segment elevation, phase 2 reentry and polymorphic ventricular tachycardia.41 This mechanism may be responsible for the manifestation of cardiac conduction disease without BrS in the proband (**II-1**) who displayed the *SCN5A* mutation as well as *CACNB2b* polymorphism. The presence of a milder form of cardiac conduction disease without manifestations of BrS in his two daughters is likely due to their young age and female gender, as discussed above. The presence of the *CACNB2b* polymorphism in one daughter (**III-1**) may have contributed to less severe conduction defect. The appearance of bifid T waves and QTc prolongation in the proband during exercise is consistent with a greater gain of function of I_{Ca} expected to be carried by the calcium channel polymorphism due to increased levels of circulating catecholamines during exercise (Figure 2B). Both daughters, one carrying the *CACNB2b* polymorphism and the other not, are likely protected from BrS by virtue of their female gender and young age.

Trafficking and Rescue

It is not clear why the P1008S mutation leads to the failure of the channels to reach the plasma membrane, and why this trafficking defect could be rescued by incubation of the transfected cells at room temperature, but not with mexiletine. Trafficking defects are thought to involve misfolding or improper assembly of the protein structure, leading to its retention in the endoplasmic reticulum and degradation without transport to the Golgi complex by the "quality control" system, in which lectin-like endoplasmic reticulum chaperones play a key role.42 Substitution of proline with serine has significant implications with respect to protein folding, and therefore, trafficking abnormalities and degradation. Specifically, insertion of a proline residue in place of the serine is likely to cause a sharp bend in the amino acid chain. Tertiary post-translational processing may be affected and thereby alter trafficking to the cell membrane.

The restoration of trafficking of mutant proteins is an experimental and therapeutic goal in protein trafficking-deficient inherited diseases, where the concept of chemical or pharmacological chaperones has emerged. Exposure to low temperature is thought to improve channel biogenesis by stabilizing the channel protein in a configuration that facilitates proper trafficking and may thus be effective in rescuing mutations that are not influenced by pharmacological agents.

Finally, using the Luo and Rudy cardiac action potential (AP) model,21 we demonstrate that the reduction in I_{Na} can cause loss of the right ventricular epicardial AP dome in the absence but not in the presence of the slowed inactivation of I_{Ca}. Slowed conduction was present in both cases.

Limitations and Conclusion

Our results suggest that genetic variations leading to a loss of function in I_{Na} coupled with a gain of function in I_{Ca} may underlie the development of cardiac conduction disease without Brugada syndrome. However, the small number of affected individuals in this family precludes us from reaching a definitive conclusion.

Supplementary Material

Refer to Web version on PubMed Central for supplementary material.

Acknowledgments

The authors are grateful to Judy Hefferon and Robert J. Goodrow, Jr. for technical assistance and Susan Bartkowiak for maintaining our genetic database.

Financial Support: This work was supported by the National Institutes of Health grant HL47678 (CA) and New York State and Florida Grand Lodges of Free and Accepted Masons.

Reference List

1. Chen Q, Kirsch GE, Zhang D, Brugada R, Brugada J, Brugada P, Potenza D, et al. Genetic basis and molecular mechanisms for idiopathic ventricular fibrillation. Nature. 1998; 392:293–296. [PubMed: 9521325]
2. Abriel H, Cabo C, Wehrens XH, Rivolta I, Motoike HK, Memmi M, Napolitano C, et al. Novel arrhythmogenic mechanism revealed by a long-QT syndrome mutation in the cardiac Na^+ channel. Circ Res. 2001; 88:740–745. [PubMed: 11304498]
3. Schott JJ, Alshinawi C, Kyndt F, Probst V, Hoorntje TM, Hulsbeek M, Wilde AA, et al. Cardiac conduction defects associate with mutations in SCN5A. Nat Genet. 1999; 23:20–21. [PubMed: 10471492]
4. Benson DW, Wang DW, Dyment M, Knilans TK, Fish FA, Strieper MJ, Rhodes TH, et al. Congenital sick sinus syndrome caused by recessive mutations in the cardiac sodium channel gene (SCN5A). J Clin Invest. 2003; 112:1019–1028. [PubMed: 14523039]
5. Olson TM, Michels VV, Ballew JD, Reyna SP, Karst ML, Herron KJ, Horton SC, et al. Sodium channel mutations and susceptibility to heart failure and atrial fibrillation. JAMA. 2005; 293:447–454. [PubMed: 15671429]
6. Bezzina C, Veldkamp MW, van Den Berg MP, Postma AV, Rook MB, Viersma JW, Van Langen IM, et al. A single Na^+ channel mutation causing both long-QT and Brugada syndromes. Circ Res. 1999; 85:1206–1213. [PubMed: 10590249]
7. Veldkamp MW, Wilders R, Baartscheer A, Zegers JG, Bezzina CR, Wilde AA. Contribution of sodium channel mutations to bradycardia and sinus node dysfunction in LQT3 families. Circ Res. 2003; 92:976–983. [PubMed: 12676817]
8. Grant AO, Carboni MP, Neplioueva V, Starmer CF, Memmi M, Napolitano C, Priori SG. Long QT syndrome, Brugada syndrome, and conduction system disease are linked to a single sodium channel mutation. J Clin Invest. 2002; 110:1201–1209. [PubMed: 12393856]
9. Makita N, Behr E, Shimizu W, Horie M, Sunami A, Crotti L, Schulze-Bahr E, et al. The E1784K mutation in SCN5A is associated with mixed clinical phenotype of type 3 long QT syndrome. J Clin Invest. 2008; 118:2219–2229. [PubMed: 18451998]
10. Van Norstrand DW, Valdivia CR, Tester DJ, Ueda K, London B, Makielski JC, Ackerman MJ. Molecular and functional characterization of novel glycerol-3-phosphate dehydrogenase 1 like

gene (GPD1-L) mutations in sudden infant death syndrome. Circulation. 2007; 116:2253–2259. [PubMed: 17967976]

11. Antzelevitch C, Pollevick GD, Cordeiro JM, Casis O, Sanguinetti MC, Aizawa Y, Guerchicoff A, et al. Loss-of-function mutations in the cardiac calcium channel underlie a new clinical entity characterized by ST-segment elevation, short QT intervals, and sudden cardiac death. Circulation. 2007; 115:442–449. [PubMed: 17224476]
12. Watanabe H, Koopmann TT, Le Scouarnec S, Yang T, Ingram CR, Schott JJ, Demolombe S, et al. Sodium channel b1 subunit mutations associated with Brugada syndrome and cardiac conduction disease in humans. J Clin Invest. 2008; 118:2260–2268. [PubMed: 18464934]
13. Delpón E, Cordeiro JM, Núñez L, Thomsen PEB, Guerchicoff A, Pollevick GD, Wu Y, et al. Functional effects of *KCNE3* mutation and its role in the development of Brugada syndrome. Circ Arrhythm Electrophysiol. 2008; 1:209–218. [PubMed: 19122847]
14. Hu D, Barajas-Martinez H, Burashnikov E, Springer M, Wu Y, Varro A, Pfeiffer R, et al. A mutation in the b3 subunit of the cardiac sodium channel associated with Brugada ECG phenotype. Circ Cardiovasc Genet. 2009; 2:270–278. [PubMed: 20031595]
15. Yan GX, Antzelevitch C. Cellular basis for the Brugada syndrome and other mechanisms of arrhythmogenesis associated with ST segment elevation. Circulation. 1999; 100:1660–1666. [PubMed: 10517739]
16. Fish JM, Antzelevitch C. Role of sodium and calcium channel block in unmasking the Brugada syndrome. Heart Rhythm. 2004; 1:210–217. [PubMed: 15851155]
17. Smits JP, Eckardt L, Probst V, Bezzina CR, Schott JJ, Remme CA, Haverkamp W, et al. Genotype-phenotype relationship in Brugada syndrome: electrocardiographic features differentiate SCN5A-related patients from non-SCN5A-related patients. J Am Coll Cardiol. 2002; 40:350–356. [PubMed: 12106943]
18. Antzelevitch C. Brugada syndrome. PACE. 2006; 29:1130–1159. [PubMed: 17038146]
19. Remme CA, Wilde AA, Bezzina CR. Cardiac sodium channel overlap syndromes: different faces of *SCN5A* mutations. Trends Cardiovasc Med. 2008; 18:78–87. [PubMed: 18436145]
20. Herfst LJ, Potet F, Bezzina CR, Groenewegen WA, Le MH, Hoorntje TM, Demolombe S, et al. Na $^{+}$ channel mutation leading to loss of function and non-progressive cardiac conduction defects. J Mol Cell Cardiol. 2003; 35:549–557. [PubMed: 12738236]
21. Luo CH, Rudy Y. A dynamic model of the cardiac ventricular action potential. I. Simulations of ionic currents and concentration changes. Circ Res. 1994; 74:1071–1096. [PubMed: 7514509]
22. Zeng J, Laurita KR, Rosenbaum DS, Rudy Y. Two components of the delayed rectifier K^{+} current in ventricular myocytes of the guinea pig type. Theoretical formulation and their role in repolarization. Circ Res. 1995; 77:140–152. [PubMed: 7788872]
23. Dumaine R, Towbin JA, Brugada P, Vatta M, Nesterenko DV, Nesterenko VV, Brugada J, et al. Ionic mechanisms responsible for the electrocardiographic phenotype of the Brugada syndrome are temperature dependent. Circ Res. 1999; 85:803–809. [PubMed: 10532948]
24. Brown, L.; Clark, BJ.; Morrow, C. Clinical Handbook of Pediatrics. 3 ed.. New York, NY: Lippincott Williams & Wilkins; 2003.
25. Robertson GA, January CT. HERG trafficking and pharmacological rescue of LQTS-2 mutant channels. Handb Exp Pharmacol. 2006:349–355. [PubMed: 16610352]
26. Tan BH, Valdivia CR, Rok BA, Ye B, Ruwaldt KM, Tester DJ, Ackerman MJ, et al. Common human SCN5A polymorphisms have altered electrophysiology when expressed in Q1077 splice variants. Heart Rhythm. 2005; 2:741–747. [PubMed: 15992732]
27. Tan HL, Bink-Boelkens MT, Bezzina CR, Viswanathan PC, Beaufort-Krol GC, van Tintelen PJ, van Den Berg MP, et al. A sodium-channel mutation causes isolated cardiac conduction disease. Nature. 2001; 409:1043–1047. [PubMed: 11234013]
28. Wang DW, Viswanathan PC, Balser JR, George AL Jr, Benson DW. Clinical, genetic, and biophysical characterization of SCN5A mutations associated with atrioventricular conduction block. Circulation. 2002; 105:341–346. [PubMed: 11804990]
29. Shaw RM, Rudy Y. Electrophysiologic effects of acute myocardial ischemia: a theoretical study of altered cell excitability and action potential duration. Cardiovasc Res. 1997; 35:256–272. [PubMed: 9349389]

30. Royer A, van Veen TA, Le BS, Marionneau C, Griol-Charhbili V, Leoni AL, Steenman M, et al. Mouse model of SCN5A-linked hereditary Lenegre's disease: age-related conduction slowing and myocardial fibrosis. Circulation. 2005; 111:1738–1746. [PubMed: 15809371]

31. Bezzina CR, Rook MB, Groenewegen WA, Herfst LJ, van der Wal AC, Lam J, Jongsma HJ, et al. Compound heterozygosity for mutations (W156X and R225W) in SCN5A associated with severe cardiac conduction disturbances and degenerative changes in the conduction system. Circ Res. 2003; 92:159–168. [PubMed: 12574143]

32. Shimizu W, Matsuo K, Kokubo Y, Satomi K, Kurita T, Noda T, Nagaya N, et al. Sex hormone and gender difference--role of testosterone on male predominance in Brugada syndrome. J Cardiovasc Electrophysiol. 2007; 18:415–421. [PubMed: 17394456]

33. Yokokawa M, Noda T, Okamura H, Satomi K, Suyama K, Kurita T, Aihara N, et al. Comparison of long-term follow-up of electrocardiographic features in Brugada syndrome between the *SCN5A*-positive probands and the *SCN5A*-negative probands. Am J Cardiol. 2007; 100:649–655. [PubMed: 17697823]

34. Cordeiro JM, Barajas-Martinez H, Hong K, Burashnikov E, Pfeiffer R, Orsino AM, Wu YS, et al. Compound heterozygous mutations P336L and I1660V in the human cardiac sodium channel associated with the Brugada syndrome. Circulation. 2006; 114:2026–2033. [PubMed: 17075016]

35. Tan BH, Valdivia CR, Song C, Makielski JC. Partial expression defect for the SCN5A missense mutation G1406R depends on splice variant background Q1077 and rescue by mexiletine. Am J Physiol Heart Circ Physiol. 2006; 291:H1822–H1828. [PubMed: 16632547]

36. Hu D, Viskin S, Oliva A, Carrier T, Cordeiro JM, Barajas-Martinez H, Wu Y, et al. Novel mutation in the *SCN5A* gene associated with arrhythmic storm development during acute myocardial infarction. Heart Rhythm. 2007; 4:1072–1080. [PubMed: 17675083]

37. Viswanathan PC, Balser JR. Molecular basis of isolated cardiac conduction disease. Handb Exp Pharmacol. 2006:331–347. [PubMed: 16610351]

38. Brugada R, Brugada J, Antzelevitch C, Kirsch GE, Potenza D, Towbin JA, Brugada P. Sodium channel blockers identify risk for sudden death in patients with ST-segment elevation and right bundle branch block but structurally normal hearts. Circulation. 2000; 101:510–515. [PubMed: 10662748]

39. Kyndt F, Probst V, Potet F, Demolombe S, Chevallier JC, Baro I, Moisan JP, et al. Novel SCN5A mutation leading either to isolated cardiac conduction defect or Brugada syndrome in a large French family. Circulation. 2001; 104:3081–3086. [PubMed: 11748104]

40. Fish JM, Antzelevitch C. Cellular and ionic basis for the sex-related difference in the manifestation of the Brugada syndrome and progressive conduction disease phenotypes. J Electrocardiol. 2003; 36:173–179. [PubMed: 14716629]

41. Antzelevitch C, Fish JM. Therapy for the Brugada syndrome. Handb Exp Pharmacol. 2006:305–330. [PubMed: 16610350]

42. Zhou Z, Gong Q, Epstein ML, January CT. HERG channel dysfunction in human long QT syndrome. Intracellular transport and functional defects. J Biol Chem. 1998; 273:21061–21066. [PubMed: 9694858]

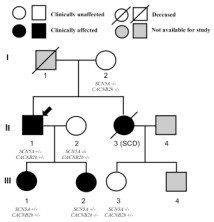

Figure 1. Pedigree of the family with *SCN5A*-P1008S mutation

Circles represent female subjects and squares represent male subjects. The arrow denotes the proband. Diagonal bars indicate deceased family members. −/− WT; +/− heterozygous for the *SCN5A*-P1008S mutation or *CACNB2b*-D601E polymorphism. SCD = Sudden Cardiac Death.

A: Patient II-1 (at rest)

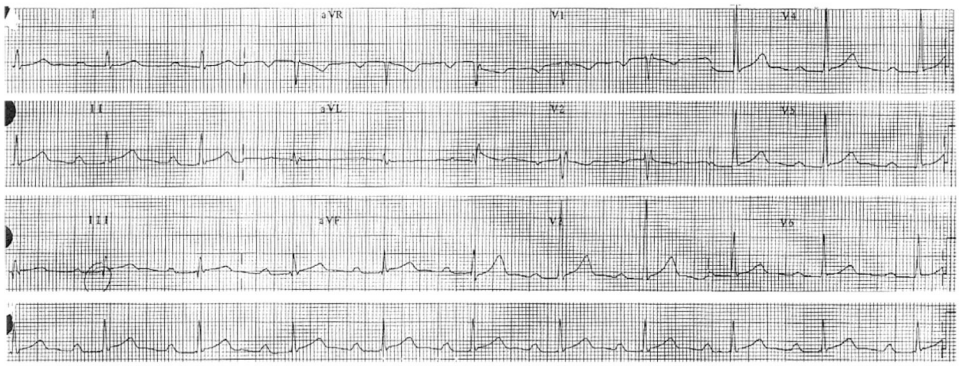

B: Patient II-1 (during stress test)

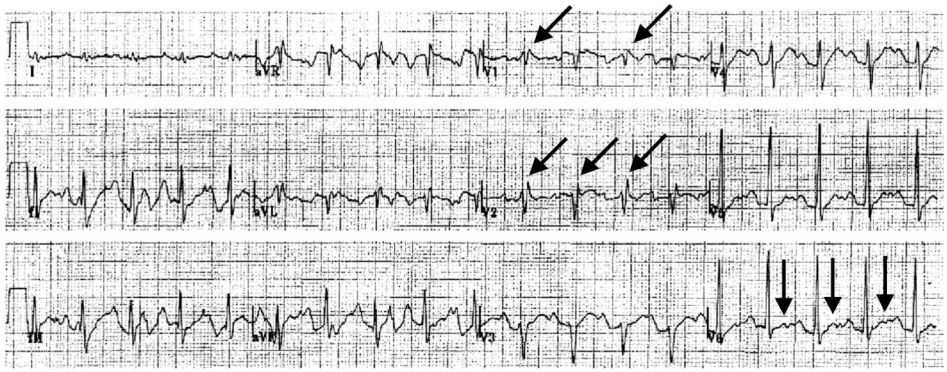

C: Patient II-1 (after stress test)

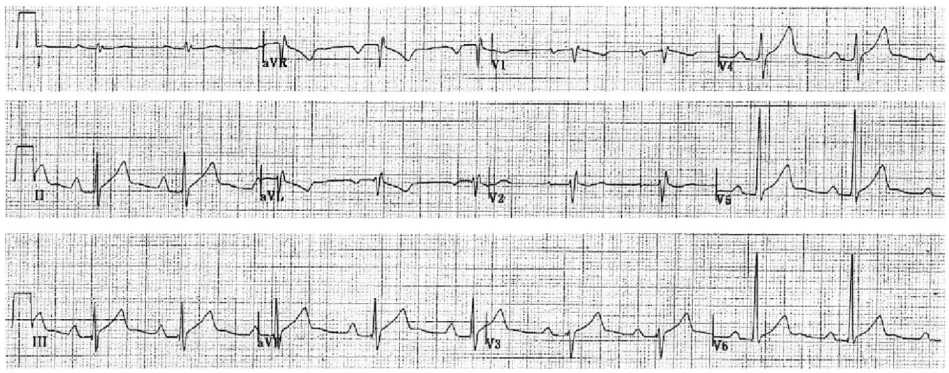

D: Patient III-1 (at rest)

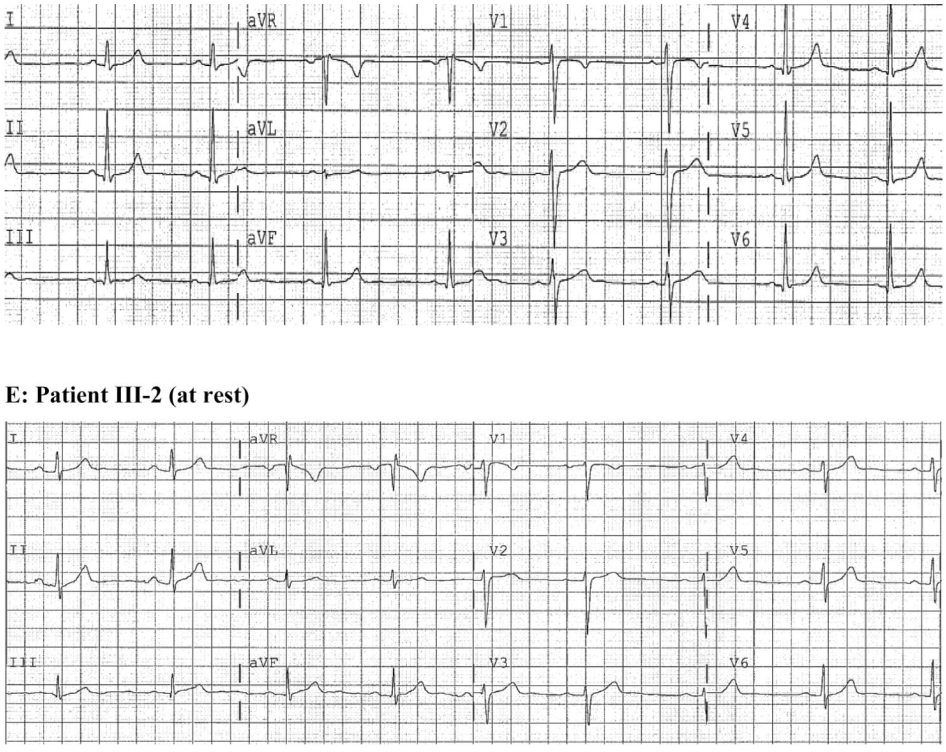

Figure 2. Corresponding representative ECGs of *SCN5A*-P1008S mutant carriers

A. ECG of the index patient (II-1) at rest shows 1st degree AV block associated with incomplete right bundle branch block (IRBBB). **B.** Recorded from proband during stress test. ECG shows accentuation of R' in right precordial leads suggestive of accentuation of IRBBB as well as the development of bifid T waves in the left precordial leads and enlarged P waves. **C.** Following the stress test, his heart rate returned to 60 bpm, although P wave and r' in V_2 remain enlarged and QTc is slightly prolonged. **D.** ECG of proband's 15 year old daughter (patient III-1) shows a PR interval of 178 ms (borderline first degree AV block) and bradycardia (HR, 51 bpm). **E.** ECG of proband's 13 yr. old daughter (patient III-2) shows 1st degree AV block, bradycardia, and sinus arrhythmia.

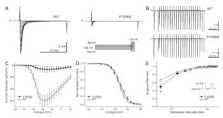

Figure 3. Comparison of electrophysiological characteristics in *SCN5A*-WT and *SCN5A*-P1008S Channels

A: Representative steady-state inactivation traces from both WT and mutant channels observed in response to the voltage clamp protocol depicted in the inset. **B:** Representative traces showing recovery from fast inactivation of WT and P1008S Na^+ channels. The two-pulse protocol is shown in the inset of panel E. Pulses were of 20 ms duration. **C:** Current density-voltage relationship for WT (open circles, n = 33) and P1008S (filled circles, n = 15). The current amplitude of P1008S was significantly reduced compared to WT at test potentials between −50 mV and 0 mV (P ≤0.001 for – 50 to −10 mV; P < 0.01 25 for −5 mV; P < 0.05 for 0 mV). **D:** Steady-state inactivation in WT and P1008S channels. $V_{1/2}$ = −92.53 ± 1.02 mV and k = 5.24 ± 0. 90 mV for WT (open circles, n = 17), and $V_{1/2}$ = − 91.16 ± 2.04 mV and k = 6.66 ± 0.81 mV for P1008S (filled circles, n = 10, P > 0.05 and P > 0.05 for differences in $V_{1/2}$ and k. **E:** Time constants of recovery from fast inactivation plotted on a log scale. Peak current elicited during the second pulse was normalized to the value obtained during the initial test pulse. **p* < 0.001, compared two groups at the same interpulse intervals. Fitting to a double-exponential function yielded the time constants as follows: τ_f = 9.32 ± 1.27 ms, τ_s= 30.95 ± 2.54 ms for WT (open circles, n = 55); τ_f = 14.55 ± 3.37 ms, τ_s = 31.65 ± 6.78 ms for P1008S (filled circles, n = 11); τ_f and τ_s were not significantly different as compared to WT.

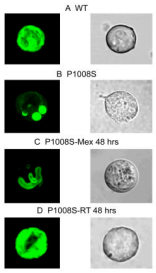

Figure 4. Confocal fluorescence microscopic images of GFP-tagged *SCN5A* channel proteins

TSA201 cells were transfected with GFP-tagged-*SCN5A* (WT or mutant P1008S) and *SCN1B*. All GFP signals were recorded 48 hours after transfection. Left and right photomicrographs show the confocal and phase contrast light transmission images, respectively, for the same cell. **A:** WT channels conjugated to green fluorescent protein showed prominent staining in both the periphery and the center of the cell suggesting that WT channels are trafficked to the cell membrane. **B:** P1008S channels showed that staining is localized in the perinuclear region of the cell, suggesting that mutant channels fail to traffic to the membrane. **C:** 48 hours incubation of the mutant P1008S with 300 μM mexiletine failed to rescue the channel. **D:** These trapped P1008S channels were rescued by incubation at room temperature.

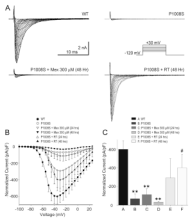

Figure 5. Rescue of *SCN5A*-P1008S channels

A: Representative sodium current traces recorded from WT, P1008S, P1008S incubated with mexiletine (300 μM) treatment and P1008S incubated at 22°C. All were recorded at 48 hours after transfection. Mexiletine was washed out 30 minutes prior to recording the traces. I_{Na} was elicited by depolarizing pulses ranging from −90 mV to +30 mV in 5 mV increments (holding potential=−120 mV). The inset on top depicts the voltage-clamp protocol employed. **B:** Current density-voltage relationship for WT (open circles, n = 33), P1008S (filled circles, n=15), P1008S incubated with 300 μM mexiletine (24 hours, open down-triangles, n=10; 48 hours, filled down-triangles, n=9) and P1008S incubated at 22°C (24 hours, open up-triangles, n = 8; 48 hours, filled up-triangles, n=11). **C:** Summary of I_{Na} amplitudes in WT, and in P1008S under control and after 24 or 48 hrs incubation with either 300 μM mexiletine or room temperature. All incubations were done at 37°C except for the room temperature group. (**P<0.01 and $^{\#}$,*P<0.05).

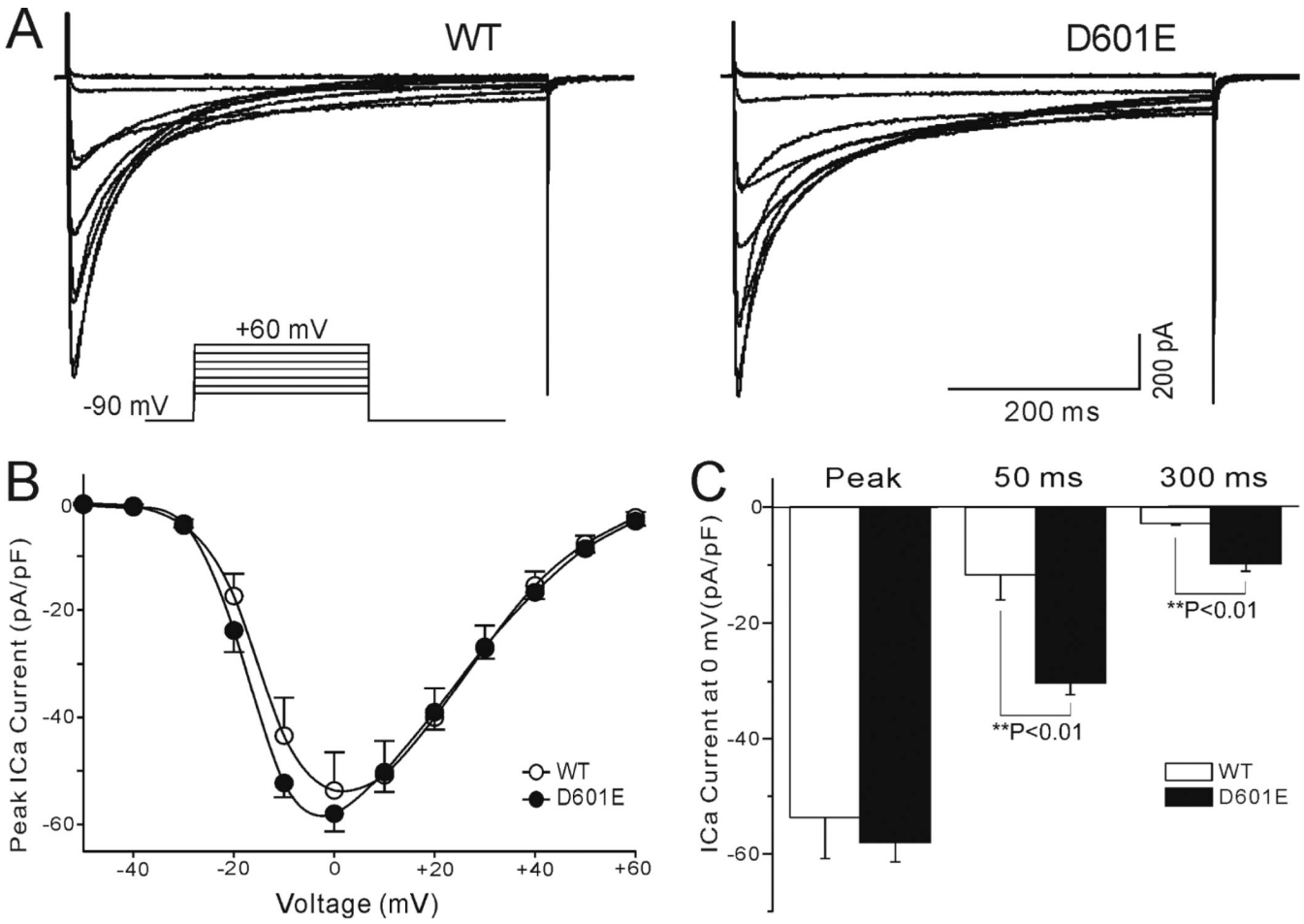

Figure 6. Electrophysiological characteristics of *CACNB2b*-D601E cardiac calcium channel polymorphism

A: Whole-cell patch-clamp current recorded from calcium WT ($\alpha_{1C}/\beta_{2A}/\alpha_2\delta$) and D601E channels in response to the voltage clamp protocol depicted as inset. **B:** Current density-voltage relationship for WT (open circles, n = 8) and D601E (filled circles, n = 7) in TSA201 cell line. **C:** Vertical bar graph of current density in 3 different time points at the voltage of 0mV. There was no significantly difference of peak current density amplitude between WT and D601E (P>0.05), but distinct difference were observed in 50 ms and 300 ms (**P<0.01).

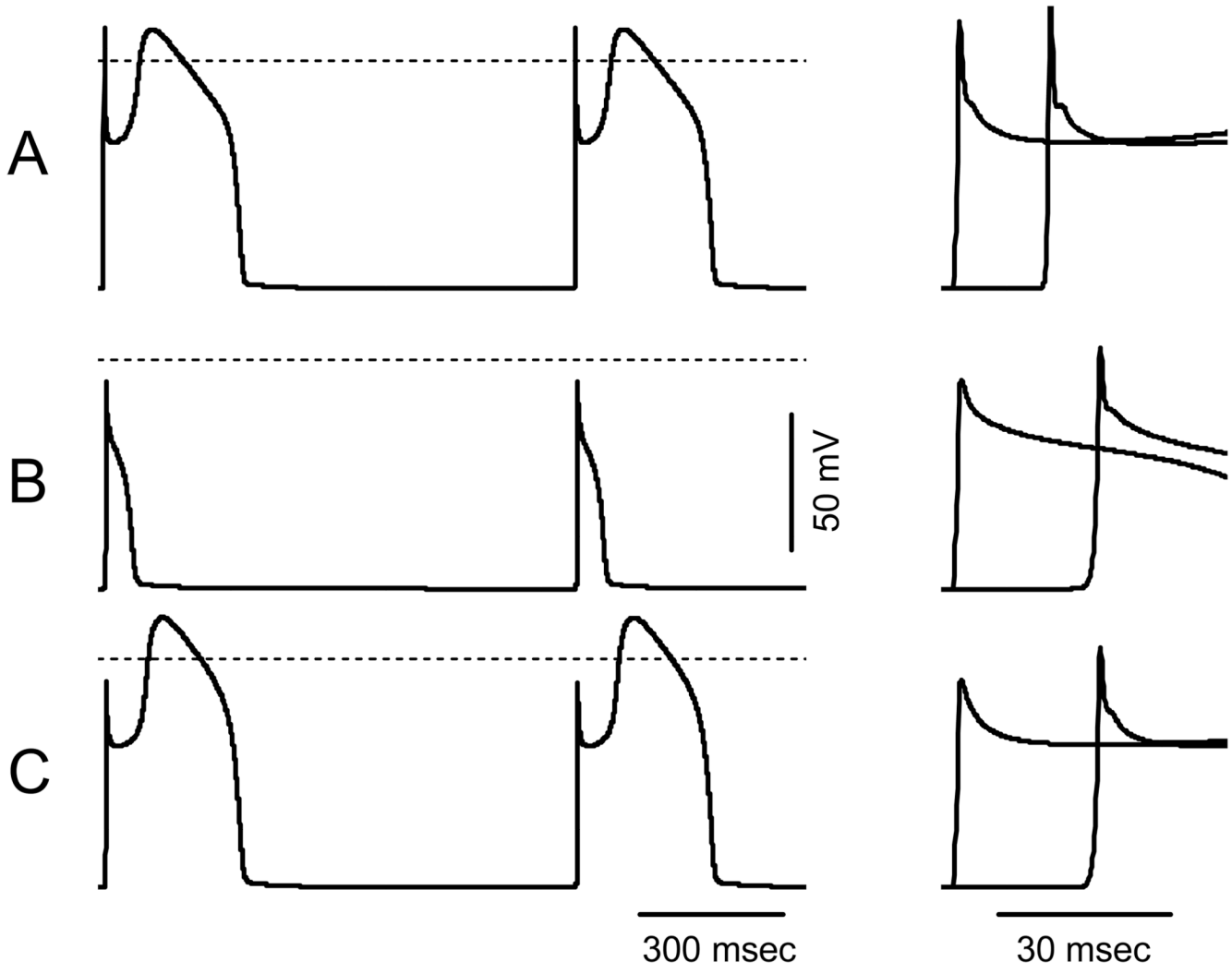

Figure 7. Propagated right ventricular APs simulated in 1 cm cable using LR2

A: WT I_{Na} and $I_{Ca,L}$. **B:** I_{Na} with P1008S mutation (G_{Na} reduced to 35% of WT). **C:** I_{Na} with P1008S-*SCN5A* mutation and I_{CaL} D601E-*CACNB2b* variant (Rate of voltage-dependent inactivation of I_{CaL} reduced to 85% of WT). Left panels show steady state (9^{th} and 10^{th}) APs from the center of the cable. Right panels show APs at the first and the last nodes of the cable at an expanded time scale to illustrate the change in the propagation velocity. Dashed lines indicate the zero potential.

Table 1

ECG Characteristics of Affected Family Members

Patient	Age (year)	Gender	Heart Rate (bpm)	P Wave Duration (ms)	PR interval (ms)	QRS Duration (ms)	QT interval (ms)	QTc interval (ms)
II-1	47	Male	60	130	300–360	105	400	400
II-1 After stress test			60	160	280	120	440	440
III-1	15	Female	51	100	178	104	440	406
III-2	13	Female	50	120	224	85	412	376